

RESEARCH ARTICLE | SEPTEMBER 15 2008

Effects of laser pulse duration on extreme ultraviolet spectra from double optical gating ✓

Steve Gilbertson; Hiroki Mashiko; Chengquan Li; Eric Moon; Zenghu Chang

*Appl. Phys. Lett.* 93, 111105 (2008)<https://doi.org/10.1063/1.2982589>View
OnlineExport
Citation

CrossMark

Articles You May Be Interested In

High Power Fibre-Integrated Supercontinuum Sources

AIP Conference Proceedings (October 2008)

Invited Article: Multiple-octave spanning high-energy mid-IR supercontinuum generation in bulk quadratic nonlinear crystals

APL Photonics (June 2016)

Separation of photonic crystal waveguides modes using femtosecond time-of-flight

Appl. Phys. Lett. (November 2002)

500 kHz or 8.5 GHz?
And all the ranges in between.

Lock-in Amplifiers for your periodic signal measurements



Find out more



Effects of laser pulse duration on extreme ultraviolet spectra from double optical gating

Steve Gilbertson, Hiroki Mashiko, Chengquan Li, Eric Moon, and Zenghu Chang^{a)}

J. R. Macdonald Laboratory, Department of Physics, Kansas State University, Manhattan, Kansas 66506, USA

(Received 28 July 2008; accepted 26 August 2008; published online 15 September 2008)

Previously a two-color field was combined with a polarization gating to allow for the generation of single isolated attosecond pulses from multicycle lasers. Here, the scaling of energy for the extreme ultraviolet pulses corresponding to single attosecond pulses as a function of input laser pulse duration was investigated for argon, neon, and helium gas. Laser pulses as long as 12 fs were able to generate extreme ultraviolet supercontinua with high photon flux. The spectra profile depended strongly on the carrier envelope phase of the pump laser. © 2008 American Institute of Physics. [DOI: 10.1063/1.2982589]

Single isolated attosecond pulses have been produced by high-order harmonic generation (HHG) using carrier envelope (CE) phase stabilized few-cycle laser pulses through a variety of methods.^{1–5} In one of them, the pump laser is linearly polarized and only the cutoff region of the harmonic spectrum is filtered out.^{2–4} Therefore, the technique requires extremely short pump pulses to produce broad spectra in the cutoff region. The energy of the 80 as pulses at center photon energy of 80 eV was 500 pJ from a neon gas target using 3.3 fs, 500 μ J pump pulses. This corresponds to a conversion efficiency of 10^{-6} .⁴ Conversely, the polarization gate technique could generate single attosecond pulses covering the plateau and cutoff regions.^{5,6} However, due to the depletion of the target gas from the circularly polarized leading edge of the pulse, the conversion efficiencies of HHG from argon and neon gas using 5 fs pump pulses were very low.

Recently HHG with two-color fields has been extensively studied since its original demonstration.^{7–11} The two-color gating process has been used in the study of both attosecond pulse trains^{12,13} and single attosecond pulses.¹⁴ In our previous work, double optical gating (DOG), combining a two-color gate with polarization gate, generated extreme ultraviolet (XUV) supercontinua.¹⁵ This technique produced both supercontinuum spectra and high photon flux even from long input pulses. In this letter, we demonstrate the scaling of harmonic photon flux versus input pulse durations.

The 8–12 fs pump pulses were generated by compressing 2 mJ, 30 fs pulses from a chirped pulse amplifier (CPA) at 1 kHz with a hollow-core fiber/chirped mirror combination.¹⁶ The input pulse duration was adjusted by changing the gas pressure in the hollow-core fiber and was measured by frequency resolved optical gating. The CE phase of the oscillator of the CPA system was locked by the self-referencing technique, and the slow drift in the amplifier was compensated through feedback control of the grating separation.^{17–19} Previously, DOG was demonstrated by a collinear setup.²⁰ The DOG field was constructed by two birefringent quartz plates and a barium borate (BBO) crystal. A linearly polarized input pulse was split into two perpendicularly polarized pulses by a quartz plate with its optic axis oriented 45° to the input polarization. The second quartz

plate had its slow axis aligned parallel to the input polarization, while the BBO had its slow axis perpendicular to the input polarization. Together they act as a quarter wave plate turning the pulses from the first quartz plate into two counter-rotating pulses. The BBO also generates the second harmonic field for the two-color gating.

Figure 1(a) shows the different values of delay between the two circularly polarized IR pulses as a function of the laser pulse duration. The solid line shows the conditions where the polarization gate width is one full cycle of 2.5 fs—the basic requirement for DOG. The dashed line in the upper left shows the conditions under which regular polarization gating is valid, i.e., a half optical cycle gate width. These calculations come from the gate width equation found in Ref. 21. DOG allows the use of longer input pulses and less delay introduced by the first quartz plate, both of which are advantages. The filled circles on the plot show the conditions at which we observed the double optical gated XUV spectra for this letter. These are 270, 350, 440, and 530 μ m with corresponding laser pulse durations of 8.2, 9.5, 10.6, and 11.7 fs, respectively. In all cases, the second quartz plate thickness was chosen as 180 μ m and the BBO crystal thickness was 60 μ m. This combination was able to produce a quarter cycle delay to produce the polarization gating field that can be resolved into a driving and a gating field.²⁰ Physically, using thinner first quartz plates and shorter durations allows for higher photon flux due to the increased driving field amplitude within the polarization gate as seen in Fig. 1(b). The ratios of the peak electric field strength of the linear portion of the pulse to the circular portion of the pulse for each quartz plate are plotted in Fig. 1(c). Ideally, the strength of the linear portion should be higher than that of the circular portion to avoid the large depletion.

The input beam with constant 750 μ J energy and various pulse durations as measured by frequency resolved optical gating was focused by a spherical mirror onto a 1.4 mm target gas cell. The Rayleigh lengths are longer than 6 mm. The peak intensities within the gate for 8.2, 9.5, 10.6, and 11.7 fs pulses were 1.7, 1.4, 1.1, and 0.9×10^{15} W/cm², respectively, at the laser focal point. The generated harmonics then passed through a 0.2 μ m thick aluminum filter used for filtering out the residual fundamental pulse. After this, the photon flux was measured by an XUV photodiode. The har-

^{a)}Electronic mail: chang@phys.ksu.edu.

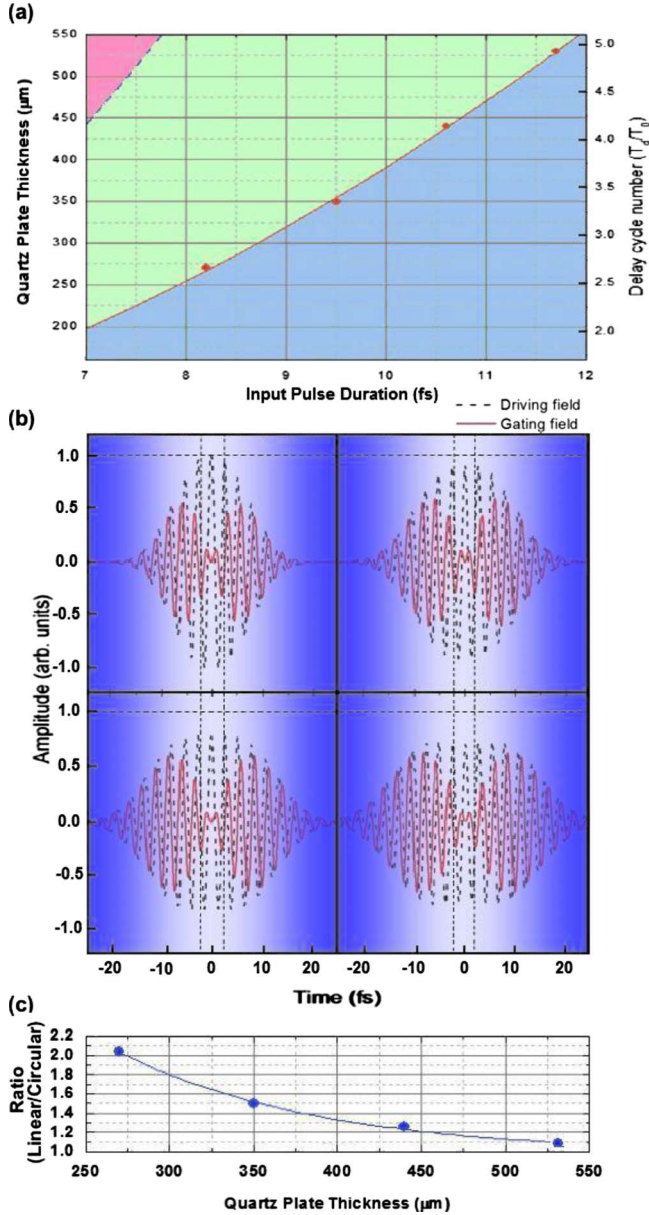


FIG. 1. (Color online) (a) The first quartz plate thickness vs input pulse duration for gate widths of 1 optical cycle (solid line) for DOG and $\frac{1}{2}$ optical cycle (dashed line) for polarization gate. The closed circles are the points that were tested. (b) Field components for the parameters chosen in (a). The solid line is the gating field and the dashed line is the driving field. The vertical dashed lines indicate the gate width in each case, while the horizontal dashed line is used to indicate the decrease in the linear portion field strength for each case. The shaded region indicates the ellipticity of the total field. (c) The ratio of the linear portion of the gate width to the maximum circular portion of the leading edge of the pulses for each case in (b).

monics were separated by an off axis toroidal grating and focused onto a microchannel plate and phosphor screen for detection.

The ability of DOG to produce broad XUV continuous spectra covering the plateau and cutoff harmonics can be seen in Fig. 2(a). Here we show typical harmonic spectral marginal plots with 10^3 integrated laser shots from argon gas while the CE phase was locked. Each plot was varied by optimizing the maximum photon flux. The procedures of optimization considered are the gas pressure dependence and the gas cell location for the propagating beam under phase matching conditions as described in Ref. 22. The notable

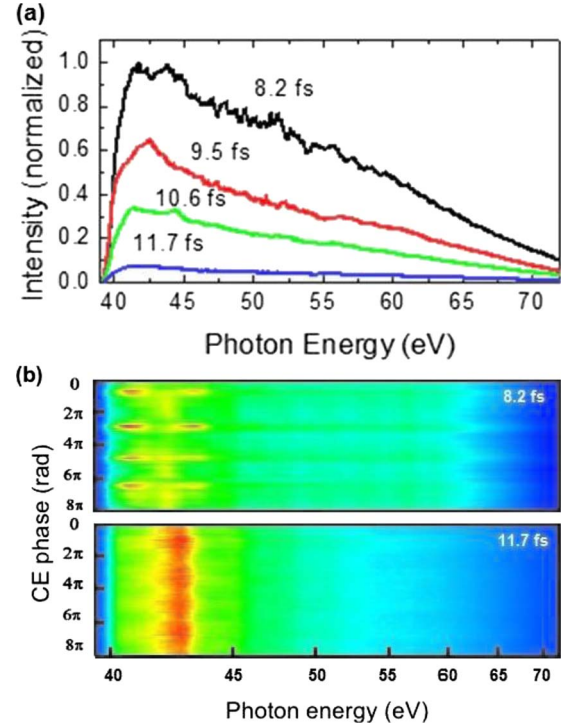


FIG. 2. (Color online) (a) Spectra of the harmonic supercontinuum generated with DOG from the different values of input pulse duration for an argon target gas. (b) The CE phase scans of the spectra for the cases of 8.2 and 11.7 fs pulses.

feature is that the thinnest quartz plates give the highest photon flux in agreement with theoretical predictions. The estimated pulse energies from the 8.2, 9.5, 10.6, and 11.7 fs pulses were 6.5, 3.7, 2.1, and 0.42 nJ, respectively. The decreased signal for the longest pulse durations as compared with the shorter durations stems from the increased target gas depletion and reduced laser intensity inside the polarization gate as described earlier. However, these values are substantially larger than the values reported earlier from polarization gating using 5 fs lasers.⁵ Figure 2(b) shows typical harmonic spectra undergoing a CE phase scan for 8.2 and 11.7 fs input pulses. The 2π periodicity can be observed in agreement with theoretical predictions even for input pulses as long as ~ 12 fs.²³

Since a main goal of this approach is to generate broad spectra capable of supporting shorter single sub-100-as pulses,⁴ neon as a target gas is an obvious choice due to its larger ionization potential. Figure 3(a) shows the spectral marginal plots of a neon target with 10^4 CE phase locked laser shots. In these results, the broad spectra are capable of supporting ~ 120 as pulse durations in the transform limited case. Here, the measured XUV pulse energies were 170, 100, 60, and 40 pJ from shortest to longest input pulse durations, respectively. Figure 3(b) shows intensity plots of the harmonic spectra as a function of the CE phase. Again, the modulation shows a 2π periodicity even for the 12 fs input pulses.

Finally, we were able to also generate spectra from a helium target gas. Figure 4(a) shows the spectra with 3×10^4 CE phase locked laser shots for each pulse duration. The right edge in the plots is the transmission cutoff of the aluminum filter. The XUV pulse energies for this case were estimated as 45, 33, 25, and 16 pJ from shortest to longest

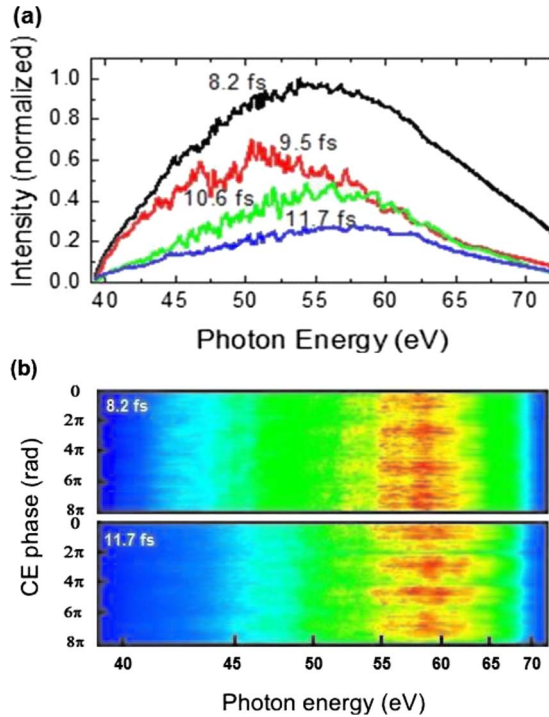


FIG. 3. (Color online) (a) Spectra of the harmonic supercontinuum generated with DOG from the different values of input pulse duration for a neon target gas. (b) The CE phase scans of the spectra for the cases of 8.2 and 11.7 fs pulses.

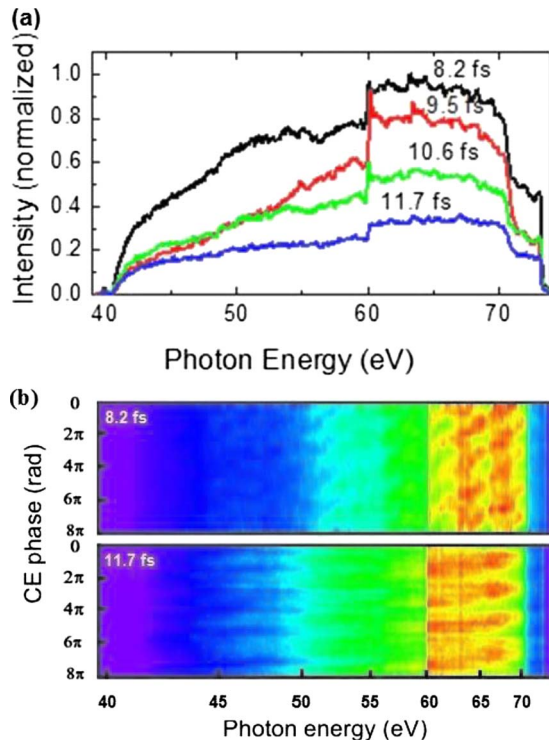


FIG. 4. (Color online) (a) Spectra of the harmonic supercontinuum generated with DOG from the different values of input pulse duration for a helium target gas. (b) The CE phase scans of the spectra for the cases of 8.2 and 11.7 fs pulses.

input pulse durations, respectively. The prominent peak in the spectra lies at ~ 60 eV. This feature corresponds to the $2s2p$ autoionization state. Only continuous spectra could show this as it lies right at an edge of a discrete order for long input pulses and would probably not be observed as noticeably under those conditions. We finally show CE phase scans with 2π periodicity in Fig. 4(b) for helium gas for the cases of 8.2 and 11.7 fs pulses.

In conclusion, it was demonstrated that DOG can be implemented with a broad range of laser pulse durations (8–12 fs). There is a tradeoff between the conversion efficiency and the laser pulse duration, but it indicates that DOG should allow single isolated attosecond pulses to be generated with high power laser systems that are unable to easily generate sufficiently short pulses for conventional polarization gating or spectrum filtering.

This material is supported by the NSF under Grant No. 0457269, the U. S. Army Research Office under Grant No. W911NF-07-1-0475, and the U.S. Department of Energy, under grant DE-FG02-86ER13491.

- ¹A. Scrinzi, M. Yu Ivanov, R. Kienberger, and D. M. Villeneuve, *J. Phys. B* **39**, R1 (2006).
- ²M. Schultze, E. Goulielmakis, M. Uiberacker, M. Hofstetter, J. Kim, D. Kim, F. Krausz, and U. Kleineberg, *New J. Phys.* **9**, 243 (2007).
- ³R. Kienberger, E. Goulielmakis, M. Uiberacker, A. Baltuska, V. Yakovlev, F. Bammer, A. Scrinzi, Th. Westerwalbesloh, U. Kleineberg, U. Heinzmann, M. Drescher, and F. Krausz, *Nature (London)* **427**, 817 (2004).
- ⁴E. Goulielmakis, M. Schultze, M. Hofstetter, V. S. Yakovlev, J. Gagnon, M. Uiberacker, A. L. Aquila, E. M. Gullikson, D. T. Attwood, R. Kienberger, F. Krausz, and U. Kleineberg, *Science* **320**, 1614 (2008).
- ⁵I. Sola, E. Mevel, L. Elouga, E. Constant, V. Strelkov, L. Poletto, P. Villaresi, E. Benedetti, J. P. Caumes, S. Stagira, C. Vozzi, G. Sansone, and M. Nisoli, *Nat. Phys.* **2**, 319 (2006).
- ⁶G. Sansone, E. Benedetti, F. Calegari, C. Vozzi, L. Avaldi, R. Flammini, L. Poletto, P. Villaresi, C. Altucci, R. Velotta, S. Stagira, S. De Silvestri, and M. Nisoli, *Science* **314**, 443 (2006).
- ⁷M. D. Perry and J. K. Crane, *Phys. Rev. A* **48**, R4051 (1993).
- ⁸H. Eichmann, A. Egbert, S. Nolte, C. Momma, B. Wellegehausen, W. Becker, S. Long, and J. K. McIver, *Phys. Rev. A* **51**, R3414 (1995).
- ⁹U. Andiel, G. D. Tsakiris, E. Cormier, and K. Witte, *Europhys. Lett.* **47**, 42 (1999).
- ¹⁰T. T. Liu, T. Kanai, T. Sekikawa, and S. Watanabe, *Phys. Rev. A* **73**, 063823 (2006).
- ¹¹I. J. Kim, G. H. Lee, S. B. Park, Y. S. Lee, T. K. Kim, C. H. Nam, T. Mocek, and K. Jakubczak, *Appl. Phys. Lett.* **92**, 021125 (2008).
- ¹²N. Dudovich, O. Smirnova, J. Levesque, Y. Mairesse, M. Yu Ivanov, D. M. Villeneuve, and P. B. Corkum, *Nat. Phys.* **2**, 781 (2006).
- ¹³J. Mauritsson, P. Johnsson, E. Gustafsson, A. L'Huillier, K. J. Schafer, and M. B. Gaarde, *Phys. Rev. Lett.* **97**, 013001 (2006).
- ¹⁴Y. Oishi, M. Kaku, A. Suda, F. Kannari, and K. Midorikawa, *Opt. Express* **14**, 7230 (2006).
- ¹⁵H. Mashiko, S. Gilbertson, C. Li, S. Khan, M. Shakya, E. Moon, and Z. Chang, *Phys. Rev. Lett.* **100**, 103906 (2008).
- ¹⁶H. Mashiko, C. M. Nakamura, C. Li, E. Moon, H. Wang, J. Tackett, and Z. Chang, *Appl. Phys. Lett.* **90**, 161114 (2007).
- ¹⁷E. Moon, C. Li, Z. Duan, J. Tackett, K. L. Corwin, B. R. Washburn, and Z. Chang, *Opt. Express* **14**, 9758 (2006).
- ¹⁸C. Li, E. Moon, and Z. Chang, *Opt. Lett.* **31**, 3113 (2006).
- ¹⁹Z. Chang, *Appl. Opt.* **45**, 8350 (2006).
- ²⁰S. Gilbertson, H. Mashiko, C. Li, S. Khan, M. Shakya, E. Moon, and Z. Chang, *Appl. Phys. Lett.* **92**, 071109 (2008).
- ²¹B. Shan, S. Ghimire, and Z. Chang, *J. Mod. Opt.* **52**, 277 (2005).
- ²²H. Mashiko, S. Gilbertson, C. Li, E. Moon, and Z. Chang, *Phys. Rev. A* **77**, 063423 (2008).
- ²³Z. Chang, *Phys. Rev. A* **76**, 051403(R) (2007).